ELSEVIER

Helical Diffraction from Tubular Structures

Lu-Chang Qin
JST-ICORP Nanotubulite Project, c/o NEC Corporation, 34 Miyukigaoka, Tsukuba, Ibaraki 305, Japan

An electron diffraction technique is described that enables both the calculation of electron diffraction intensity distribution from a given tubule structure and the deduction of its true helicity from an experimental electron diffraction pattern of the nanotube. The cylindricality and the helicity of nanotubes are taken into full account. An example of the applications is also presented as an illustration for the simulation of the electron diffraction pattern and the deduction of its true helicity of a single-walled helical carbon nanotube of indices [12, 1].

INTRODUCTION

The unique properties of carbon nanotubes [1–3] have made this new form of solid carbon a most studied nanomaterial for the past few years. A striking characteristic of carbon nanotubes is that they can behave either as a metal or as a semiconductor, depending on their diameter and helicity, as has been demonstrated both theoretically and experimentally [4–9]. The one-dimensionality property has turned carbon nanotubes to an ideal quantum wire model material for studies of many low-dimensional phenomena [10, 11]. In the aspect of microstructural characterization, many morphological studies have been reported using various microscopy techniques, including transmission electron microscopy (TEM), scanning electron microscopy (SEM), and scanning probe microscopies (SPM). TEM techniques have many unique features, and have been most powerful in obtaining structural information of nanotubes on the atomic scale, in particular on individual tubules and aggregates such as raft-like bundles. On the one hand, various electron imaging techniques are able to provide direct visualization of the tubule diameters and their variations in real space. On the other hand, electron diffraction techniques provide complementary information on the helicities of nanotubes.

The electron diffraction techniques are useful in two major aspects for the study of the helical nature of carbon nanotubes: (a) revealing the helical characteristic of nanotubes, and (b) determining the true helicity of the nanotubes. So far, electron diffraction is still the only technique that allows one to identify and to deduce the helicity of carbon nanotubes, in particular for the multiwalled tubules, where the capability of scanning probe microscopies is limited to identifying the outmost layer at best. However, transmission electron diffraction is able to examine all layers in a multiwalled nanotube simultaneously.

In the present paper, the methodology for both the calculation of diffraction patterns from a known tubule structure and the deduction of the true helicity of the tubule from an experimental electron diffraction pattern is presented. An application of the technique is illustrated with a practical [12, 1] single-walled carbon nanotube as an example.

STRUCTURE DESCRIPTION

Figure 1 shows schematically how a well-defined single-walled carbon nanotube is described crystallographically from a section of graphene. Once the crystallographic basis vectors are defined (in this paper, the crystallographic convention [12] is adopted where the interangle between the two basis

MATERIALS CHARACTERIZATION 44:407–412 (2000)

655 Avenue of the Americas, New York, NY 10010
1044-5803/00/$–see front matter
PII S1044-5803(00)00057-7

vectors is 120°), the tubule perimeter can be described by a vector [u, v], and the tubule axis perpendicular to the perimeter is also well defined. Given in Fig. 1(a) is the crystallographic definition of basis vectors $\mathbf{a}_1$ and $\mathbf{a}_2$, and Fig. 1(b) is the electron diffraction pattern from the graphene shown in Fig. 1(a). The radial projection of the [12, 1] tubule is shown in Fig. 1(c), and a single-walled carbon nanotube formed by rolling up this section is shown in Fig. 1(d).

When the indices [u, v] are given, the tubule diameter d is given by

$$d = \frac{a_0}{\pi}(u^2 + v^2 - uv)^{1/2},$$

where $a_0 = 0.2451$nm is the lattice constant of the graphene net, and the helical angle α, defined as the angle between the basis vector $\mathbf{a}_1$ and the perimeter vector, is given by

$$\alpha = \cos^{-1}\left[\frac{2u - v}{2(u^2 + v^2 - uv)^{1/2}}\right].$$

RESULTS AND DISCUSSION

CALCULATION OF SCATTERING AMPLITUDE

The scattering amplitude for a given single-walled carbon nanotube of radius r can be calculated using the following equation [12]:

$$F(R,\Phi,l) = \sum_{n=-\infty}^{+\infty} B_n(R,\Phi)T_{nl},$$

where

$$B_n(R,\Phi) = \exp\left[in\left(\Phi + \frac{\pi}{2}\right)\right]J_n(2\pi rR)$$

accounts for the cylindricality of the tubule in which $J_n(u)$ is the Bessel function of order n and

$$T_{nl} = \sum_j f_j \exp\left[i\left(n\phi_j + \frac{2\pi l z_j}{C}\right)\right] = \sum_j f_j \exp\left[2\pi i\left(\frac{nx_j}{A} + \frac{lz_j}{C}\right)\right]$$

expresses the electron scattering amplitude from a repetitive unit of the tubule in radial projection, where f_j is the atomic scattering amplitude for the atom positioned at cylindrical coordinates (r_j, ϕ_j, z_j), (R, Φ, Z) are the cylindrical coordinates in reciprocal space, and A and C are the perimeter and the periodicity along the tubule axis, respectively.

Figure 2 shows the calculated electron diffraction intensity distribution from a single-walled carbon tubule of indices [12, 1] using the above equations.

A noteworthy feature in the electron diffraction pattern is that the cylindricality of

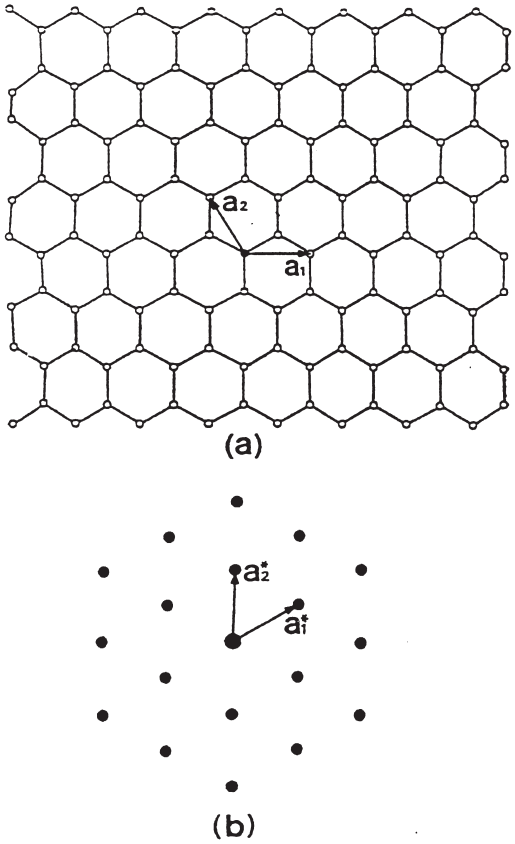

FIG. 1. Choice of basis vectors to define the crystallographic indices and schematic showing the structure of a [12, 1] tubule made out of a graphene. (a) Basis vectors $\mathbf{a}_1$ and $\mathbf{a}_2$ in a graphene net with an interangle of 120°; (b) corresponding electron diffraction pattern from the graphene oriented in (a); (c) radial projection of a repetitive structural unit of the [12, 1] tubule; and (d) section of the finished [12, 1] single-walled carbon nanotube.

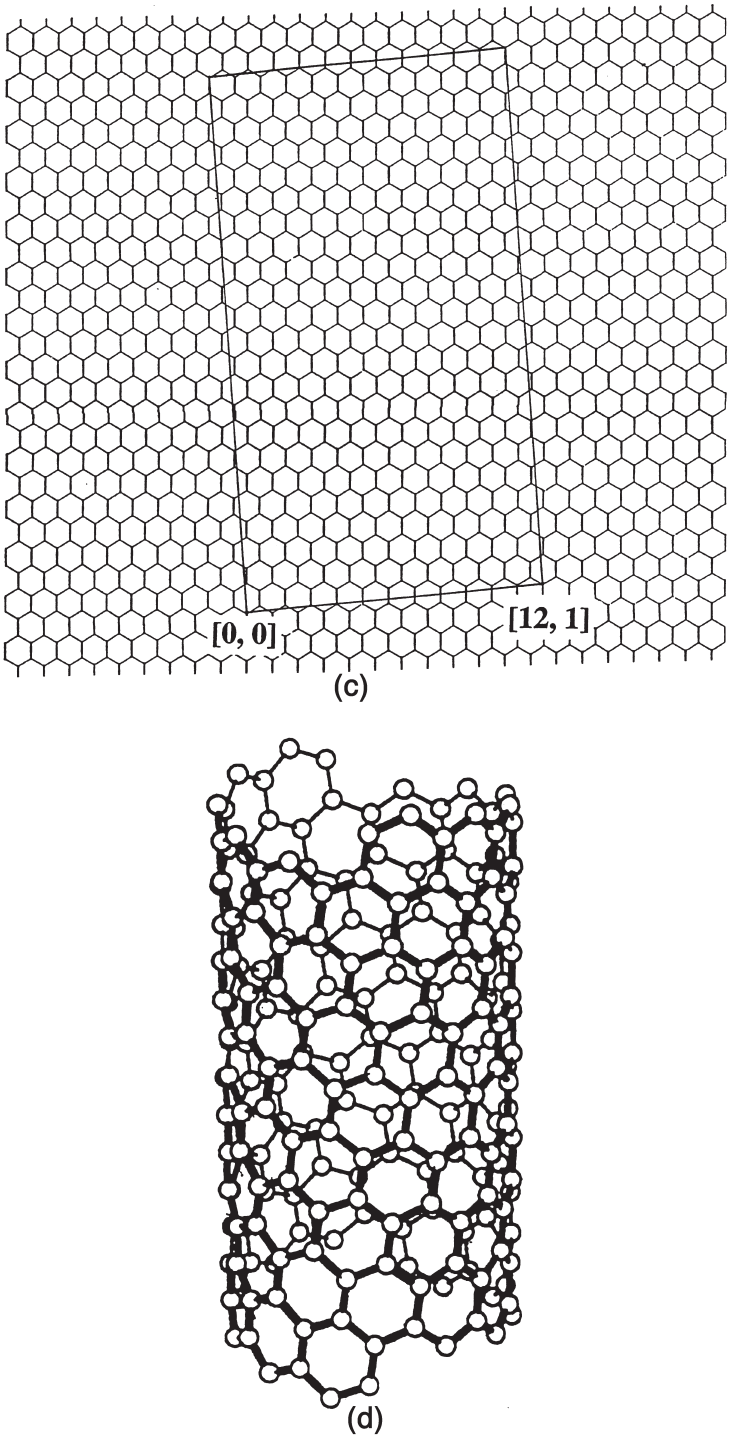

FIG. 1. Continued

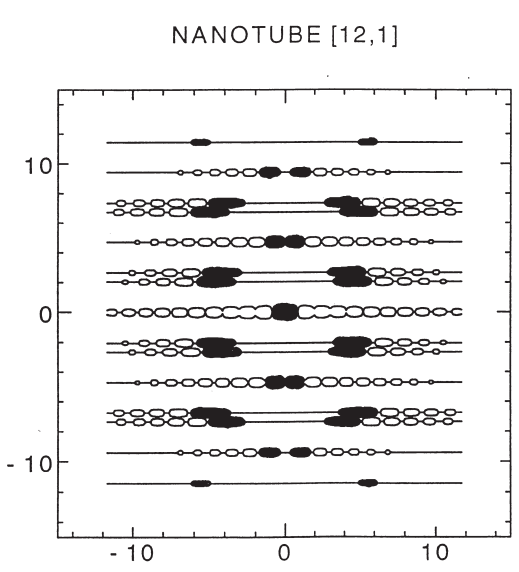

FIG. 2. Calculated electron diffraction intensity map for the single-walled carbon nanotube of indices [12, 1]. The scale is in nm^{-1}.

the nanotube results in significant geometry changes in the diffraction pattern. This effect (referred to as cylindrical effect hereafter) can no longer be neglected to obtain accurate results. This effect is stronger for smaller helical angles, as the cylindrical distortion is, to a large extent, dictated by the relevant Bessel functions. As has been shown [13], the distortion can be rather large for low order Bessel functions. For example, when $n = 1$, the correction factor can be as large as 80%.

DEDUCTION OF TRUE HELICITY

As discussed above, the cylindricality of a nanotube causes distortion in the diffraction pattern. This change of symmetry is reflected by the difference between the true helical angle α and the half-twist angle θ, which is the half-angle of rotation between the two sets of graphene diffraction patterns resulting from the respective top and bottom layers of a single-walled carbon nanotube. This distortion needs to be accounted for to deduce the true helicity of a nanotube. The distortion, which is in effect to enlarge the separation between the graphene reflections and is governed by the dominating Bessel function, can be expressed in the following equation [13]:

$$\tan(\theta_n) = \frac{u_n}{n}\tan(\alpha),$$

where u_n is the value of the variable for which the nth order Bessel function $J_n(u)$ assumes its first maximum. The values of u_n/n are known as cylindrical correction factors.

When the (010) reflection is used for zigzag tubules ($0 \leqslant \alpha \leqslant 15°$) and the (110) reflection for armchair tubules ($15° \leqslant \alpha \leqslant 30°$) for the measurement of the twist angle with respect to the tubule axis, fortunately the correction factor u_n/n can be linked to the helical angle α in a very straightforward way [14]:

$$\begin{cases} n = v, \text{ for } (0 \leqslant \alpha \leqslant 15°,) \\ n = -u + 2v, \text{ for } (15° \leqslant \alpha \leqslant 30°.) \end{cases}$$

This simple relationship makes it a fairly easy task to deduce the true helicity of a carbon nanotube from its electron diffraction patterns.

Figure 3 is an experimental electron diffraction pattern from a single-walled carbon nanotube of 0.9nm diameter [13]. The half-twist angle θ measured on the (010) reflection with respect to the tubule axis is about 7.5°, and this value fits the tubule of indices [12, 1], where the correction factor (u_n/n) is about 1.8, leading to the true helical angle $\alpha = 4.3°$.

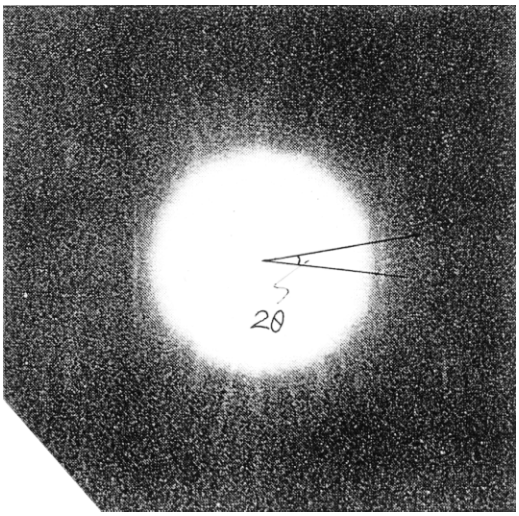

FIG. 3. Experimental electron diffraction pattern of a tubule of diameter 0.9nm. The apparent twist angle 2θ measured on the (010) reflections along the axial direction in this diffraction pattern is about 15°. The true helicity of this carbon nanotube is determined to be 4.3° with indices [12, 1].

The above development allows the accurate deduction of the true helicity of a nanotube of known diameter using an experimental electron diffraction pattern from the tubule. Figure 4 shows a flow chart of the procedure that has been used for the determination of the crystallographic indices [*u, v*] of a single-walled carbon nanotube. The tilt β refers to the angle between the tubule axis and the horizontal plane that is perpendicular to the optic axis [13], which would effectively reduce the apparent twist angle shown in the experimental electron diffraction pattern (EDP). The true value of θ refers to the value corrected for the tilting angle β. As shown previously, it should not be difficult to determine whether the tubule is of zigzag or armchair structure from the geometry of the electron diffraction pattern; this classification would actually greatly reduce the number of possible [*u, v*] values to begin with. Once the crystallographic indices [*u, v*] are determined, the helicity is also determined using Eq. (2). This procedure is valid for both the zigzag tubules and the armchair tubules, although the axial reflections used for these two cases could be different. However, it should be mentioned that the choice of using the (010) reflection for the zigzag tubules and the (110) reflection for the armchair tubules is only for the sake of experimental conveniences, because these reflections show highest reflection intensities for the two structures in respective settings.

When the single-walled carbon nanotubes form raft-like bundles [15, 16], the helicity distribution can also be elucidated using electron diffraction analysis [17, 18]. Experimental results have shown that the majority of the single-walled carbon nanotubes produced by laser evaporation have a rather random distribution of helicities instead of being single valued.

It should be noted that the above methodology is extendable to the case of multiwalled carbon nanotubes. For a multiwalled tubule, the resultant electron diffraction pattern is a superposition of the diffraction patterns from all the individual shells [19]. Because the coherence between the shells is rather weak, this superposition is a simple sum of all individual intensities to a satisfactory approximation for helicity analysis.

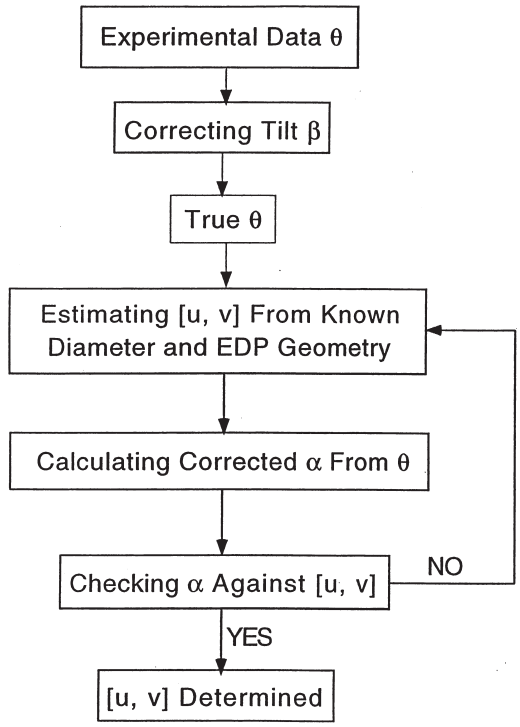

FIG. 4. Flow chart illustrating the procedure for deducing the true helicity of a carbon nanotube of known diameter from an experimental electron diffraction pattern.

CONCLUSIONS

Electron diffraction patterns from carbon nanotubes can be accurately calculated for any given structure using the helical diffraction theory for tubular structures. The cylindrical effect is taken into full account by incorporating Bessel functions into the scattering formulas. Using an experimentally obtained electron diffraction pattern, the true helicity of the diffracting carbon nanotube can be deduced after appropriate corrections are made to account for the cylindrical effect. An example has been demonstrated for the case of a [12, 1] single-walled carbon nanotube.

References

1. S. Iijima. *Nature* 354:56 (1991).
2. S. Iijima and T. Ichihashi. *Nature* 363:603 (1993).
3. D. S. Bethune, C.-H. Kiang, M. S. de Vries, G. Gorman, R. Savay, J. Vazquez, and R. Beyers. *Nature* 363:605 (1993).
4. J. W. Mintmire, B. I. Dunlop, and C. T. White. *Phys. Rev. Lett.* 68:631 (1992).
5. H. Hamada, S. Sawada, and A. Oshiyama. *Phys. Rev. Lett.* 68:1579 (1992).
6. R. Saito, M. Fujita, G. Dresselhaus, and M. S. Dresselhaus. *Appl. Phys. Lett.* 60:2204 (1992).
7. C. H. Olk and J. P. Heremans. *J. Mater. Res.* 9:259 (1994).
8. J .W. G. Wildoer, L. C. Venema, A. G. Rinzler, R. E. Smalley, and C. Dekker. *Nature* 391:59 (1998).
9. T. Wang Odom, J. L. Huang, P. Kim, and C. Lieber. *Nature* 391:62 (1998).
10. S. J. Tans, M. H. Devoret, H. Dai, A. Thess, R. E. Smalley, L. J. Geerligs, and C. Dekker. *Nature* 386: 474 (1997).
11. M. Bockrath, D. H. Cobden, P. L. McEuen, N. G. Chopra, A. Zettl, A. Thess, and R. E. Smalley. *Science* 275:1922 (1997).
12. L. C. Qin. *J. Mater. Res.* 9:2450 (1994).
13. L. C. Qin, T. Ichihashi, and S. Iijima. *Ultramicroscopy* 67:181 (1997).
14. L. C. Qin. *Chem. Phys. Lett.* 297:23 (1998).
15. A. Thess, R. Lee, P. Nikolaev, H. Dai, P. Petit, J. Robert, C. Xu, Y. H. Lee, S. G. Kim, A. G. Rinzler, D. T. Colbert, G. E. Scuseria, D. Tomanek, J. E. Fisher, and R. E. Smalley. *Science* 273:483 (1996).
16. L. C. Qin and S. Iijima. *Chem. Phys. Lett.* 269:65 (1997).
17. L. C. Qin, S. Iijima, H. Kitaura, Y. Maniwa, S. Suzuki, and Y. Achiba. *Chem. Phys. Lett.* 268:101 (1997).
18. J. M. Cowley, P. Nikolaev, A. Thess, and R. E. Smalley. *Chem. Phys. Lett.* 265:379 (1997).
19. X. F. Zhang, X. B. Zhang, G. Van Tendeloo, S. Amelinckx, M. Op de Beeck, and J. Van Landuyt. *J. Cryst. Growth* 130:368 (1993).

Received 1 October 1999; accepted 1 December 1999.